Research Square

Preprints are preliminary reports that have not undergone peer review.
They should not be considered conclusive, used to inform clinical practice,
or referenced by the media as validated information.

Salinity-Dependent PFOA Transport and Membrane Stability in a Hybrid Electrokinetic–Ion Exchange System for Produced Water

Emmanuel Mbah

emmanuel.mbah@mail.concordia.ca

Concordia University

Maria Elektorowicz

Concordia University - Sir George Williams Campus: Concordia University

Mehrab Malekshahi Nejad

Concordia University - Sir George Williams Campus: Concordia University

Research Article

Keywords: perfluorooctanoic acid (PFOA) removal, produced water, electrokinetics (EK), ion exchange membranes (IEM), salinity effects, high ionic strength

Posted Date: November 4th, 2026

DOI: https://doi.org/10.21203/rs.3.rs-11121227/v1

License: This work is licensed under a Creative Commons Attribution 4.0 International License.
Read Full License

Salinity-Dependent PFOA Transport and Membrane Stability in a Hybrid Electrokinetic–Ion Exchange System for Produced Water

Emmanuel Mbah*, Maria Elektorowicz, Mehrab Malekshahi Nejad

1. Emmanuel Mbah*
   Institution: Department of Building, Civil and Environmental Engineering, Concordia University, Montreal, QC, H3G 1M8, Canada.
   Email: emmanuel.mbah@mail.concordia.ca
   Phone: +1(438) 887-9672

2. Maria Elektorowicz
   Institution: Department of Building, Civil and Environmental Engineering, Concordia University, Montreal, QC, H3G 1M8, Canada.
   Email: mariae@encs.concordia.ca
   Phone: +1 (514) 825-2924

3. Mehrab Malekshahi Nejad
   Institution: Department of Building, Civil and Environmental Engineering, Concordia University, Montreal, QC, H3G 1M8, Canada.
   Email: mehrab.nejad@concordia.ca
   Phone: +1 (438) 680-0599

Abstract

Produced water is a challenging industrial wastewater because its high salinity and complex ionic composition can strongly influence electrically driven contaminant transport and membrane stability. This study investigated a two-stage hybrid electrokinetic–ion exchange membrane (EK–IEM) process for PFOA removal from produced water, focusing on the coupled effects of salinity, ionic transport, electrical loading, energy demand, and membrane stability. Experiments were conducted at nominal salinities of 10, 20, and 80 g NaCl/L, with initial PFOA concentrations of 12.32, 14.50, and 17.14 mg/L, respectively. Membrane-free electrokinetic pretreatment substantially reduced oil, chemical oxygen demand, and turbidity before membrane treatment. Subsequent EK–IEM treatment achieved PFOA removals of 99.5%, 96.3%, and 97.5% under low-, medium-, and high-salinity conditions, respectively. Increasing salinity increased electrical current and thermal loading while substantially increasing specific energy consumption. At the highest salinity, physical rupture of the anion exchange membrane was observed under the condition that also exhibited the highest electrical and thermal loading. The results indicate that salinity creates a trade-off between ionic transport, PFOA removal, energy demand, and membrane stability. Rather than removal efficiency alone, these coupled factors should therefore be considered when defining the operating window of EK–IEM treatment for hypersaline PFAS-contaminated wastewater.

Keywords: perfluorooctanoic acid (PFOA) removal, produced water, electrokinetics (EK), ion exchange membranes (IEM), salinity effects, high ionic strength

1. Introduction

1.1 Problem statement

Per- and polyfluoroalkyl substances (PFAS), including perfluorooctanoic acid (PFOA) and perfluorooctane sulfonate (PFOS), are synthetic chemicals valued for their hydrophobicity and chemical stability but increasingly recognized as recalcitrant environmental pollutants (. Kwiatkowski et al., 2020). Perfluorooctanoic acid (PFOA) predominantly exists as the perfluorooctanoate anion ($PFOA^-$) under environmentally relevant pH conditions. The strong C–F bonds contribute to the exceptional thermal, chemical, and biological persistence of PFAS, resulting in its accumulation in water, soil, and living organisms (Glüge, et al., 2020). Among these compounds, perfluorooctanoic acid (PFOA) is one of the most studied due to its persistence in the environment, widespread occurrence in wastewater, and potential adverse health effects, including endocrine disruption, immunotoxicity, and carcinogenicity (Buck et al., 2011; Post et al., 2012).

Industrial activities such as fluoropolymer manufacturing, firefighting foam applications, and oil and gas extraction are major contributors to PFAS contamination in aquatic environments (Ateia et al., 2020). Produced water is often characterized by high salinity, complex organic mixtures, and variable chemical composition. Total dissolved solids (TDS) in produced water can range from 10 g/L to more than 200 g/L, making treatment particularly challenging. Recent studies of hypersaline produced water have similarly shown that high salinity and complex organic and inorganic compositions create additional challenges for membrane treatment, including increased fouling potential and energy requirements (Al-Maas et al., 2025).

Global regulations are tightening: the US Environmental Protection Agency (U.S. Environmental Protection Agency, 2024) recently established a maximum contaminant level (MCL) of 4 ppt for PFOA in drinking water, while The European Union Drinking Water Directive specifies parametric values of 0.10 µg/L for the sum of specified PFAS and 0.50 µg/L for total PFAS (European Parliament and Council of the European Union, 2020). Meeting such stringent standards requires advanced treatment technologies. To preserve high-quality water resources, Produced Water requires specific upgraded treatment before discharge.

However, the performance of electrically driven membrane treatment in hypersaline produced water cannot be evaluated from PFOA removal alone. Increasing ionic strength can simultaneously alter solution conductivity, electrical current, competing-ion transport, energy demand, and thermal loading of the membrane system. The resulting interaction between enhanced ionic conduction and membrane stability remains insufficiently understood for PFOA treatment in highly saline produced-water matrices.

1.2 Properties of perfluorooctanoic acid (PFOA) and transport behavior

Perfluorooctanoic acid (PFOA) has the molecular formula $C_7F_{15}COOH$. In aqueous systems, it can dissociate according to the acid–base equilibrium: $C_7F_{15}COOH \rightleftharpoons C_7F_{15}COO^- + H^+$
This implies that PFOA can exist either in its acidic form ($C_7F_{15}COOH$) or its anionic conjugate base ($C_7F_{15}COO^-$), depending on the pH of the surrounding environment (Du et al., 2014). Perfluorooctanoic acid (PFOA) and related per- and polyfluoroalkyl substances (PFAS) are weak acids that predominantly exist in their anionic form ($PFOA^-$) under environmentally relevant pH conditions. Their speciation is governed by acid dissociation equilibria, which strongly influence their mobility in aqueous systems.

The pKa of PFOA has been widely debated, but studies suggest that under typical environmental conditions (pH 5–8), PFOA exists almost entirely as an anion, promoting mobility in water and electrokinetic systems (Burns and Ellis, 2008; Goss, 2008). Solution chemistry, particularly the presence of multivalent cations and ionic strength, can further influence PFAS behavior through ion pairing, electrostatic shielding, and altered partitioning behavior (Du et al., 2014). Recent reviews indicate that membrane technologies provide promising PFAS separation, while hybrid membrane processes can improve treatment performance but may introduce additional energy and process-complexity considerations (Taher et al., 2024).

1.3 Environmental behavior and treatment implications

Whereas PFOA predominantly exists as an anion in most environmental waters, it is highly mobile and persistent earning the label of a “forever chemical” (Buck et al., 2011). This anionic character also explains why anion exchange resins (AERs) and other anion-targeted technologies are effective for its removal from water in lab and field conditions (Dixit et al., 2021).

Conventional methods—including granular activated carbon (GAC), reverse osmosis (RO), and advanced oxidation processes (AOPs)—are challenged by high salinity, which suppresses PFAS adsorption and increases osmotic pressure, resulting in reduced selectivity and higher operational costs (Appleman et al., 2014; Rahman et al., 2014). Produced water from oil and gas operations is particularly problematic due to its high ionic strength, presence of multivalent cations, as well as other hydrocarbons (Veil et al., 2004; Xu et al., 2019).

The hybrid electrokinetic (EK) treatment and ion exchange membranes (IEMs) have recently emerged as promising tools for contaminant removal. EK applies an electric field to move ions through porous media, while IEMs selectively transport cations or anions, enabling separation of PFAS from background electrolytes (Peng et al., 2020; Jiang et al., 2021). Although electrokinetic transport and ion-exchange membrane separation have each been investigated for ionic contaminants, their coupled application to PFOA treatment in highly saline produced water remains insufficiently characterized. Recent work has demonstrated effective electrochemical adsorption of PFOA using ion-exchange membranes, with applied potential, treatment time, and initial PFOA concentration influencing removal (Zhang and Crittenden, 2024). However, this approach focused on electrochemical adsorption in aqueous solutions rather than coupled PFOA and competing-ion transport through an EK–IEM reactor treating hypersaline produced water. Recent reviews have also identified membrane-based PFAS treatment as a rapidly developing field, while highlighting energy requirements and the need for improved hybrid and integrated processes (Taher et al., 2024). Furthermore, recent research on PFAS-contaminated hypersaline brines demonstrates that high-salinity matrices present distinct membrane-treatment challenges (Salih et al., 2026). Despite these advances, limited attention has been given to how increasing salinity simultaneously affects PFOA transport, competing-ion migration, electrical current, energy consumption, and membrane integrity in an EK–IEM system. These studies demonstrate the growing interest in treating PFAS in high-salinity streams; however, they do not address electrically driven PFOA transport through an AEM/CEM system or the associated relationship between salinity, current, energy consumption, and ion-exchange membrane stability.

This study therefore investigates a two-stage EK–IEM process for PFOA treatment of produced water across low-, medium-, and high-salinity conditions. The first stage uses membrane-free electrokinetic pretreatment to reduce oil, organic matter, and suspended or colloidal contaminants before membrane treatment. The second stage evaluates PFOA and inorganic-ion transport through the AEM/CEM configuration. The specific objectives are to: (i) quantify PFOA removal across a broad salinity range; (ii) examine how salinity influences chloride, sulfate, and PFOA transport; (iii) relate salinity-dependent current and thermal loading to energy consumption; and (iv) evaluate membrane integrity under high-salinity operation. The study uses these coupled observations to identify the operational trade-offs that govern EK–IEM treatment of PFOA in hypersaline wastewater.

1.4 Electrokinetic transport mechanisms

Electrokinetic systems rely on the application of an external electric field to induce the movement of charged species through aqueous or porous media. The primary transport mechanisms include electromigration, electroosmotic flow (EOF), and electrophoresis. Electromigration governs the directional movement of ionic species toward oppositely charged electrodes, while EOF refers to bulk fluid movement driven by the electrical double layer at solid–liquid interfaces (Acar and Alshawabkeh, 1993; Probstein and Hicks, 1993). Electrokinetic treatment has also been investigated for oil–water phase separation in oily sludge, demonstrating the potential of electrically driven processes for treating complex oily matrices (Jahromi and Elektorowicz, 2018).

1.5 Ion-exchange membrane transport and selectivity

Ion-exchange membranes (IEMs), including anion exchange membranes (AEMs), are selectively permeable materials that allow counter-ions to pass while partially excluding co-ions. This selectivity is governed by Donnan exclusion, membrane fixed-charge density, and ion partitioning behavior. Real membranes may deviate from ideal selectivity because of swelling, structural imperfections, concentration polarization, and operating conditions (Strathmann, 2004).

2. Methodology

2.1 Coupled EK–IEM transport and separation of PFOA

Under an applied electric field, PFOA migrates as an anion toward the anode, while electroosmotic flow may enhance or oppose transport depending on system configuration. The integration of electrokinetic transport theory with

membrane separation processes provides a promising framework for PFOA removal, but system performance is strongly dependent on operational conditions, including salinity, applied voltage, and membrane characteristics (Strathmann, 2004; Nikonenko et al., 2010).

2.2. Preparation of synthetic Produced Water

The synthetic produced-water matrices were prepared as designated as low-, medium-, and high-salinity conditions to reflect realistic PW conditions (LCT, MCT, and HCT), respectively. Additional salts were included in each matrix to reproduce the targeted ionic composition of produced water (Table 1). These values represent the nominal NaCl concentrations used during preparation rather than total dissolved salt concentrations. Following electrokinetic pretreatment and clarification, PFOA was added to the treated matrices at 12.32 mg/L, 14.50 mg/L, 17.14 mg/L for LCT, MCT, and HCT, respectively.

Table 1. Components and parameters of synthetic PW used in this work

Parameters	**Low conc.**	**Medium conc.**	**High conc.**
pH	5.6	5.0	3.0
Temperature ^{o}C	20	21	21
Oil/grease (mg/l)	240	240	240
Total suspended solids	1000	400	1000
PFOA (mg/L)	12.32	14.50	17.14
Salinity (mg/l)	10000	20000	80000
COD (mg/L)	1000	4500	9000
Ammonia (NH_4HCO_3) (mg/L)	30	60	120
Barium $(Ba(OH)_2$ (mg/L)	50	130	250
Boron boric acid (H_3BO_3) (mg/L)	10	25	40
Chloride (mg/L)	10000	22000	41000
Lead Pb $(NO_3)_2$ (mg/L)	0	0.47	0.92
Iron $Fe_2(SO_4)_3$ (mg/L)	300	690	1370
Calcium $CaCl_2$ (mg/L)	250	500	1100
Zinc $ZnCl_2$ (mg/L)	10	15	30
Manganese $MnSO_4$ (mg/L)	10	20	40
Sulphate (mg/L)	300	600	1200
Potassium KCl (mg/L)	500	1200	2000
Sodium NaCl (mg/L)	10000	21000	39000
Magnesium $MgCl_2$ (mg/L)	250	500	1100

2.3 Initial electrokinetic purification of Produced Water

The treatment protocol consisted of two sequential steps: (i) an initial membrane-free electrokinetic pretreatment to destabilize and remove suspended, colloidal, and oil-associated contaminants, followed by (ii) hybrid EK–IEM treatment for dissolved-ion transport and PFOA removal.

Initial electrokinetic purification was performed as a pretreatment step prior to the combined EK–IEM experiments**.** Raw produced water (PW) was introduced into an electrokinetic reactor operated without ion-exchange membranes for less than 1 h, as summarized in Table 2. The purpose of this preliminary treatment was to reduce suspended solids, colloidal matter, and oil-associated particulates that could subsequently contribute to membrane fouling or interfere with ion transport during the EK–IEM treatment.

Table 2. Results of step 1

PW samples	Voltage (V)	Time (min)	Conductivity		pH		Oil content (mg/L)		COD (mg/L)		Turbidity	
			initial	final	initial	final	initial	final	initial	final	initial	final
Low salinity	1.5	45	98	87	3.0	8.0	240	ND	1037	136	577	250
Medium salinity	1.5	32	104	90	2.5	11.2	240	ND	1147	37	845	200
High salinity	1.5	17	185	160	1.9	7.4	240	ND	2243	45	1560	300

Table 2 summarizes the results of the initial membrane-free electrokinetic pretreatment applied to the produced water prior to EK–IEM treatment. The pretreatment was performed at a constant applied voltage of 1.5 V, with optimized treatment durations of 45, 32, and 17 min for LCT, MCT, and HCT, respectively. The results demonstrate significant removal of oil, organic matter, and suspended/colloidal material. Oil concentrations decreased from 240 mg/L to below the analytical detection limit for all three salinity conditions and represented by no detection (ND) in (table 2). COD decreased by 86.9%, 96.8%, and 98.0% for LCT, MCT, and HCT, respectively, while turbidity decreased by 56.7%, 76.3%, and 80.8%, respectively.

In contrast, conductivity decreased by only 11.2%, 13.5%, and 13.5% for LCT, MCT, and HCT, respectively, indicating that the pretreatment primarily targeted suspended, colloidal, and organic contaminants rather than extensive dissolved-salt removal. Substantial increases in pH were also observed, from 3.0 to 8.0 for LCT, 2.5 to 11.2 for MCT, and 1.9 to 7.4 for HCT, reflecting electrochemically induced changes in the aqueous environment. Accordingly, the membrane-free electrokinetic treatment served as a pretreatment step, whereas the subsequent AEM/CEM-based EK–IEM stage was responsible for the controlled transport of dissolved ions and PFOA.

2.4. Electrokinetic–ion exchange membrane system setup

The treatment consisted of two sequential stages. In Stage 1, produced water underwent membrane-free electrokinetic pretreatment at 1.5 V for 45, 32, and 17 min for LCT, MCT, and HCT, respectively. After pretreatment and clarification, PFOA was added to the treated matrices at the concentrations specified in Table 1. The PFOA-containing matrices were then introduced into the central compartment (B) of the three-compartment EK–IEM reactor. Stage 2 was conducted at an applied electric-field gradient of 4 V/cm, corresponding to 40 V across the 10-cm electrode spacing, using DC power supply (Gw INSTEK GPR-11H300), stainless steel electrodes and was maintained for treatment periods of 1–5 h.

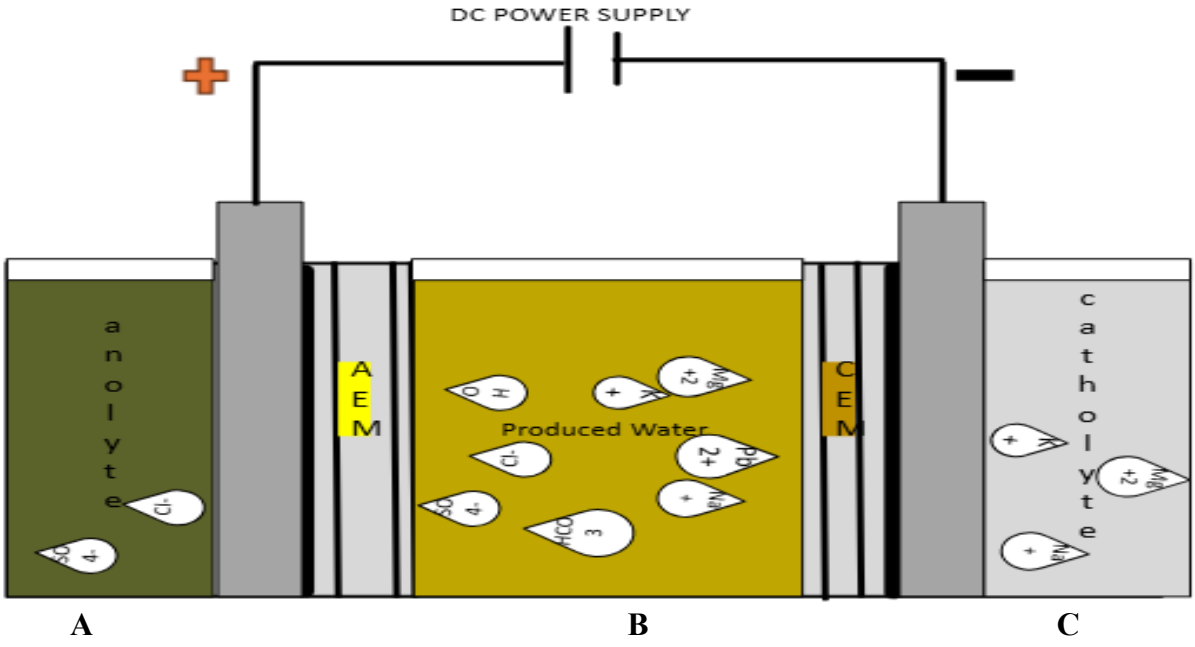


Figure 1. Schematic representation of the hybrid EK–IEM reactor. AEM, anion exchange membrane; CEM, cation exchange membrane; compartment B, central produced-water feed; compartments A and C, anolyte and catholyte receiving compartments, respectively.

2.5. Analytical methods

To assess evolution of PFOA content in the hybrid system, sampling of catholyte, anolyte and middle compartment was conducted every 1-hour interval. Prior to quantification, samples underwent a solid phase extraction (SPE) procedure adapted from EPA Method 533 (U.S. Environmental Protection Agency, 2021). A vacuum manifold and SPE cartridges were used to process the samples. The samples were filtered, diluted, and spiked with PFOA only after pretreatment.: a) conditioned the treated PFOA PW with 6 mL of methanol of each sample; b) equilibrated each sample with 6 mL of DI water; c) each sample (6 mL) was loaded in solid phase extraction; d) each loaded sample is washed with 6 mL of 2% HCOOH in H_2O; e) finally, each sample was eluted with NH_4OH (2 mL) in methanol (4 mL).

MS analyses were performed on an Agilent 1290 LC system coupled to a Thermo LTQ Orbitrap Velos mass spectrometer equipped with a heated electrospray ion source at negative mode. No analytical column was used and the mobile phase (water/acetonitrile 1:1, plus 0.1% formic acid) flowed through the system at a rate of 250 µL/min for 4 minutes per sample. 5 µL of each sample was injected and MS spectra (m/z 200-800) were acquired in the Orbitrap at a resolution of 100000. The spectra were internally calibrated using a background peak at m/z 311.1686 Da as a lock mass. PFOA was targeted as [M-H]- at m/z 412.9664. Peak intensities were reported as average values of MS Scan #3-8 using Thermo XCalibur software (v2.2 SP1.48).
PFOA concentrations were measured in triplicate (n = 3), and the reported values represent the arithmetic mean of the three measurements.

PFOA concentration was estimated using a single-point response factor based on a 5 mg/L PFOA reference standard. The mean PFOA signal intensity of the reference standard was 278,000 intensity units. Assuming proportional instrument response over the investigated concentration range, sample concentrations were estimated from the ratio of sample signal intensity to reference-standard signal intensity. Because a multi-point calibration curve and isotopically labelled internal standard were not used, the calculated concentrations should be interpreted as semi-quantitative estimates. Accordingly, the primary comparison among treatments is based on the relative PFOA removal calculated from the measured response, while the reported concentrations provide an approximate concentration scale.

Salinity and Total Dissolved Solids were measured with Oakton CON 11 portable conductivity / TDS standard meter with RS-232 Cable - WD-35607-49.

Ion chromatography (IC, Metrohm 930 Compact IC Flex) was used to quantify major inorganic anions, including chloride (Cl^-) and sulfate (SO_4^{2-}), as well as cations (e.g., Na^+, Ca^{2+}, Mg^{2+}, Ba^{2+}), which play a significant role in ion competition within the electrokinetic system.

Membrane conditions were inspected through visual inspection post-treatment and membrane morphology was examined by scanning electron microscopy (SEM) after treatment. Traceable thermometer was used for temperature measurement (-50 to 150ºC). Electrical parameters such as voltage and current were measured with DC power supply (Gw INSTEK GPR-11H300).

2.6. Statistical analysis

PFOA measurements were conducted in triplicate (n = 3 and are reported as arithmetic means. Statistical significance was not assessed because replicate raw measurements were not retained for all experimental conditions.

Removal efficiency was calculated based on the equation 1:

$$\text{Removal Efficiency (\%)} = \frac{C_0 - C_t}{C_0} \times 100 \quad \text{.....[1]}$$

where: C_0 = initial PFOA concentration (mg/L); C_t= concentration at time t (mg/L).

Converting peak intensity to mg/L (278000 is the peak intensity of 5 ppm (mg/L) PFOA standard).

$$C_{PFOA} = \frac{\text{Ct}}{278000} \text{x } 5 \times 1000 \text{ ppb} \quad \text{..... [2]}$$

$$C_{PFOA} = \frac{\text{Ct}}{278000} \text{x } 5 \left(\frac{\text{mg}}{\text{L}}\right) \quad \text{..... [3]}$$

Where: C_{PFOA} = PFOA concentration at treatment time t(mg/L), C_t= measured PFOA peak intensity at treatment time t, C_{std}= peak intensity of the PFOA reference standard (278,000), C_{std}= concentration of the PFOA reference standard (5 mg/L)

Specific energy consumption (SEC) expressed as kWh m^{-3} or kWh/L

$E=V\int I(t)dt$ ……..……. [4]

$$SEC = \frac{VI\Delta t}{1000V_{treated}} \text{ ……..…. [5]}$$

Where: V — Applied voltage (V), I — Current (A), Δt — Treatment time (h), V_{treate}d — Treated volume (mL)

3. Results and Discussion

3.1 PFOA removal as a function of treatment time

PFOA removal generally increased during the initial treatment period, although the temporal response varied among salinity conditions under the applied electric field of 4 V/cm, Under LCT, removal reached its maximum at approximately 3 h before decreasing slightly at later times, whereas MCT and HCT continued to improve through 5 h. The electric potential gradient promoted the electromigration of negatively charged PFOA molecules toward the anode compartment. As treatment progressed, the measured PFOA concentration in the central compartment generally decreased, consistent with net electrically driven transport out of the feed compartment. Because the experiments did not independently quantify membrane flux or electroosmotic flow, the concentration decrease is interpreted as net removal from the feed rather than as a direct measurement of the intrinsic PFOA flux through the AEM (Fig. 2a).

However, the removal rate gradually slowed as the concentration of PFOA in the feed compartment decreased. This behavior is consistent with electro-membrane transport processes where ion migration is governed by electric potential gradients and concentration polarization effects.

3.2. PFOA removal performance

The result showed that the EK–IEM system achieved substantial PFOA removal under all conditions (Fig. 2).

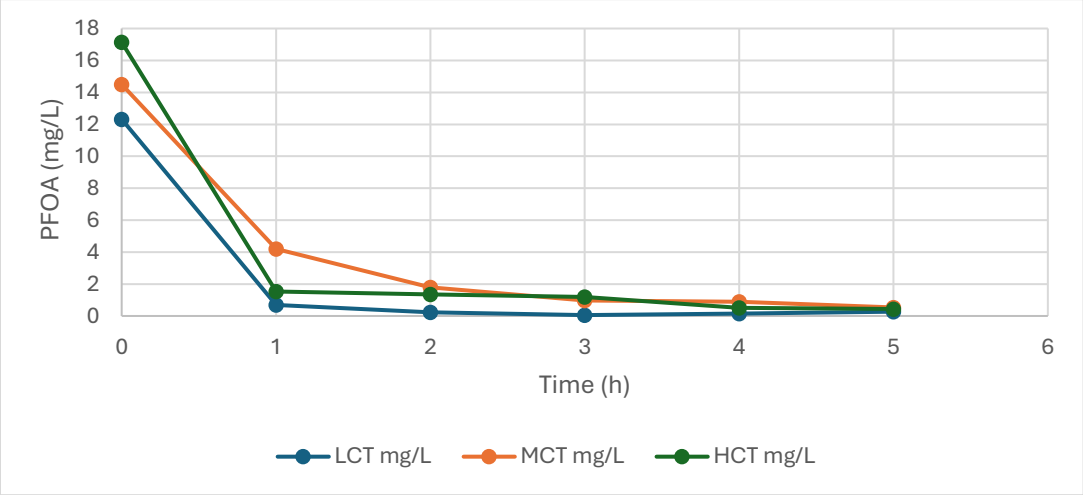


Figure 2a. **PFOA concentration change vs time and vs. salinity level: LCT (low), MCT (medium), HCT (high)**

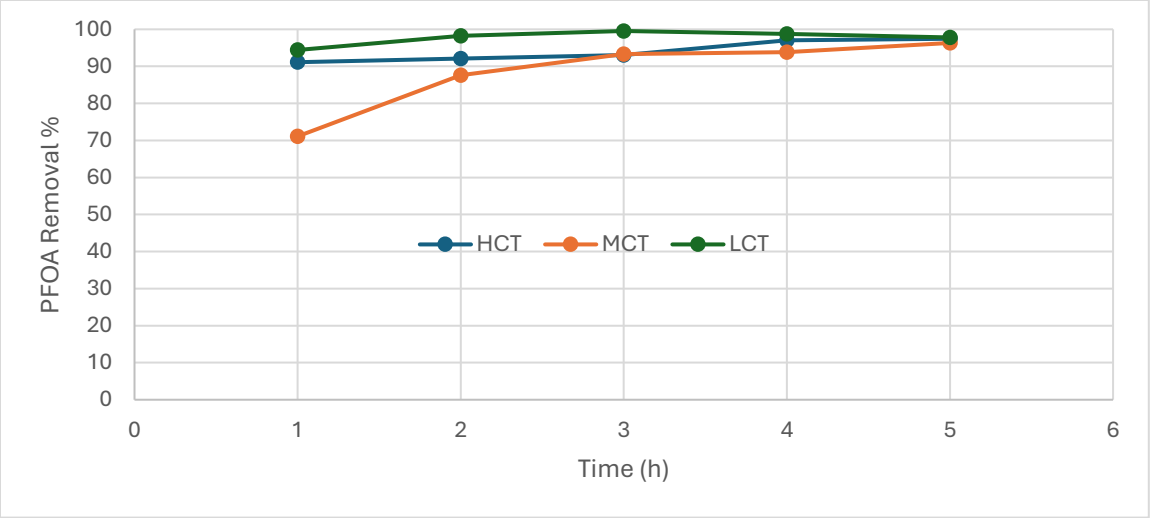


Figure 2b. PFOA removal (%) vs. time and vs. salinity level: LCT (low), MCT (medium), HCT (high)

The combined concentration and removal profiles in Fig. 2 show that the EK–IEM system maintained high PFOA removal across the investigated salinity range. Final PFOA concentrations decreased from 12.32, 14.50, and 17.14 mg/L to 0.056, 0.53, and 0.43 mg/L under LCT, MCT, and HCT, respectively, corresponding to removals of 99.5%, 96.3%, and 97.5% (Fig. 2b). Thus, increasing salinity did not eliminate PFOA removal capability, although it altered the electrical and ionic conditions under which removal occurred. Performance was highest at low salinity but remained >95% even at 80 g/L NaCl in water solution.

The relatively small difference in final PFOA removal across the three salinity conditions is notable because the ionic environment changed substantially from 10 to 80 g/L NaCl. Thus, increasing salinity did not eliminate PFOA removal capability, but it altered the electrical and transport conditions under which removal was achieved. This distinction is important because treatment performance must be evaluated together with current, energy consumption, competing-ion transport, and membrane integrity rather than from PFOA removal alone.

3.3. Salinity reduction, competing-ion and PFOA transport

The contrasting transport behavior of chloride and sulfate provides evidence that the ionic composition of the feed influenced the overall transport environment of the AEM. Chloride removal remained approximately 99% across the three salinity conditions, whereas sulfate removal decreased from 97.0% under LCT to 71.1% under MCT and 64.0% under HCT (Fig.3a and 3b)

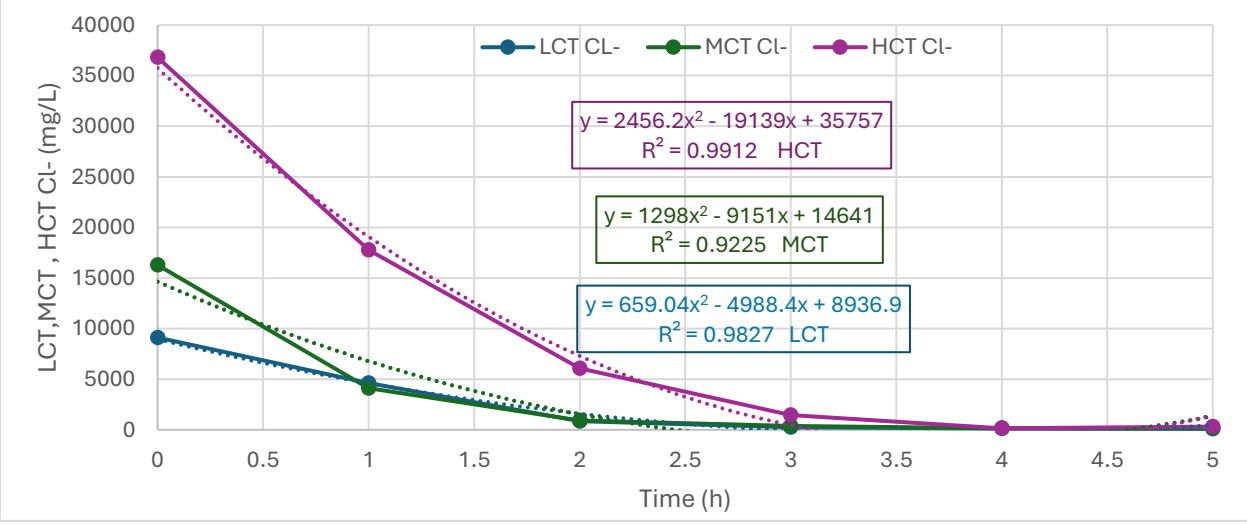


Figure 3a. Temporal evolution of chloride concentrations vs time during EK–IEM treatment under LCT, MCT, and HCT conditions

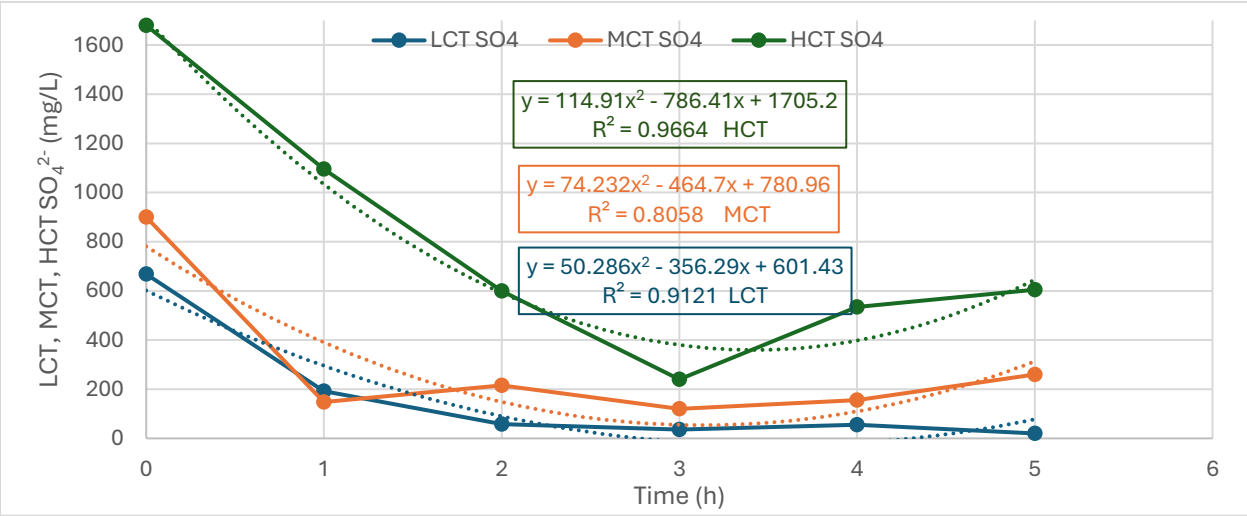


Figure 3b. Temporal evolution of sulfate concentrations vs time during EK–IEM treatment under LCT, MCT, and HCT conditions

Because chloride and sulfate were present at concentrations several orders of magnitude higher than PFOA, these inorganic ions contributed substantially to the overall ionic flux and electrical current. Their abundance therefore provides a plausible explanation for why high salinity can alter the relative contribution of PFOA to total anionic transport, even when overall PFOA removal remains high

Table 3 salinity-removal behavior and its relationship with PFOA removal

Condition	Cl^- removal at 5 h	Cl^- R^2 values	SO_4^{2-} removal at 5 h	SO_4^{2-} R^2 values
LCT	98.98%	0.9912	97.01%	0.9121
MCT	99.12%	0.9827	71.11%	0.8058
HCT	99.17%	0.9225	63.99%	0.9664

Sulfate exhibited a different transport response. Under LCT, sulfate decreased from 668 to 20 mg/L, corresponding to 97.01% removal. Under MCT and HCT, however, sulfate concentrations initially decreased before increasing during the later stages of treatment. At 5 h, sulfate removal was 71.11% for MCT and 63.99% for HCT. The lower sulfate removal at higher salinity indicates that sulfate transport was more sensitive to changes in ionic strength and competing ionic fluxes than chloride transport. The post-3-h increase in sulfate concentration may indicate redistribution, back-transport, or concentration-polarization effects during prolonged treatment.

The ion-transport behavior provides important context for the observed PFOA removal. PFOA removal efficiencies were 99.5%, 96.3%, and 97.5% for LCT, MCT, and HCT, respectively. Unlike chloride, which maintained approximately 99% removal, and sulfate, whose removal declined markedly with increasing salinity, PFOA exhibited a non-monotonic response. This indicates that PFOA transport was controlled by multiple interacting processes rather than by ionic strength alone.

The quadratic regression models provided good representations of the observed chloride and Sulfate concentration profiles, with values of 0.9912, 0.9827, and 0.9225 for LCT, MCT, and HCT, and 0.9121, 0.8058, and 0.9664 for LCT, MCT, and HCT, respectively (Fig. 3a and 3b).

Overall, the results demonstrate substantial reduction of major dissolved ions alongside PFOA removal, highlighting the coupled desalination and contaminant-removal potential of the hybrid EK–IEM system, consistent with previous reports of electrodialysis-based ion transport and salt removal (Strathmann, 2010; Xu et al., 2019; Jiang et al., 2021).

3.4. Effect of salinity on the efficiency of PFOA removal

PFOA removal remained high across the investigated salinity range, although its temporal response varied among the three conditions (Fig. 3). Increasing salinity substantially increased the concentrations of background ions, particularly chloride and sulfate, which can contribute strongly to total anionic transport through the AEM (Appleman et al., 2014; Rahman et al., 2014). Consequently, the fraction of the total ionic flux associated with PFOA may decrease as ionic strength increases, even when the absolute PFOA removal remains high. Increased ionic strength may also modify interfacial charge screening and concentration-polarization behavior. These effects provide a plausible explanation for the observed differences in PFOA transport among the salinity conditions; however, the present experiments do not independently quantify membrane transport numbers or the individual contributions of these mechanisms (Zhang et al., 2019).

3.5. Interpretation of salinity-dependent PFOA transport and membrane behavior

The transport of PFOA within the electrokinetic–ion exchange membrane (EK–IEM) system is governed by a combination of electromigration, electroosmotic flow (EOF), and ion interaction effects, while all are strongly influenced by solution chemistry and energy input and membrane-based electrochemical separations (Acar and Alshawabkeh, 1993; Nikonenko et al., 2010; Strathmann, 2004). This study considers an aqueous matrix containing PFOA at three salinity levels.

3.5.1 Electromigration at low ionic strength

Since PFOA exists predominantly as the anionic species ($PFOA^-$) and is transported primarily by electromigration toward the anode and through the AEM (Tab. 5) (Acar and Alshawabkeh, 1993; Goss, 2008). However, the present experiments quantify concentration changes rather than intrinsic membrane transport numbers; therefore, electromigration is interpreted as the dominant expected transport mechanism rather than as an independently quantified contribution. In this regime, the applied electric field promotes the migration of negatively charged $PFOA^-$ ions across the anion exchange membrane (AEM) via an electromigration-dominated transport mechanism. The fixed positively charged functional groups within the AEM facilitate the transport of anions while excluding cations, thereby enhancing the preferential transfer of $PFOA^-$ from the central feed compartment toward the anode compartment through the AEM, which is characteristic of ion-exchange membrane systems (Strathmann, 2004; Nikonenko et al., 2010). The early stages of treatment showed rapid PFOA removal (>94% at 1 h under LCT), consistent with substantial electromigration-driven transport under the low-salinity condition.

Table 4. PFOA concentrations detected in the anolyte during EK–IEM treatment. LCT- low salinity PW, MCT – medium salinity PW, HCT – high salinity PW

Treatment time (h)	LCT (mg/L)	MCT (mg/L)	HCT (mg/L)
1	0.0096	0.1720	0.0063
2	0.0034	0.0078	0.0024
3	0.0049	0.0065	0.0030
4	0.0536	0.0043	0.0091
5	0.0032	0.0069	0.0050

3.5.2 Possible contribution of electroosmotic and non-ideal transport at high salinity

As salinity increases, the high concentrations of inorganic ions such as Na^+, Cl^-, and SO_4^{2-} substantially influence charge transport and current through the system. The resulting changes in ionic strength and electrochemical conditions may promote non-ideal transport phenomena, including electroosmotic water movement and concentration-polarization effects. Such processes could contribute to the observed PFOA detected outside the expected anion-transport pathway. However, because electroosmotic flow was not measured independently in the present study, its contribution to PFOA transport cannot be quantified directly (Tab. 6) (Strathmann, 2004).

Table 5. PFOA concentrations detected in the catholyte during EK–IEM treatment. LCT- low salinity PW, MCT – medium salinity PW, HCT – high salinity PW

Treatment time (h)	LCT (mg/L)	MCT (mg/L)	HCT (mg/L)
1	0.0069	0.0189	0.0448
2	0.0173	0.0133	0.0173
3	0.0415	0.2392	0.0134
4	0.0300	0.0117	0.0183
5	0.0205	0.0099	0.0428

Chloride and sulfate were below the analytical detection limits in the catholyte, whereas PFOA was detected under several conditions. The detection of PFOA in the catholyte indicates that ideal anion electromigration alone may not fully explain the observed PFOA distribution. Possible contributors include electroosmotic water movement, concentration-polarization effects, ion association, and, importantly, non-selective passage associated with AEM damage. Because these mechanisms were not independently measured, their individual contributions cannot be distinguished from the present experiments (Zhang et al., 2013; Rahman et al., 2014).

3.5.3 Role of ion pairing and complexation

The presence of high concentrations of mono- and multivalent cations (e.g., Na^+, Ca^{2+}, Mg^{2+}, Ba^{2+}) further alters PFOA transport behavior. Previous studies suggest that mono- and multivalent cations can interact with PFOA through ion pairing and electrostatic association. Such interactions may modify the effective charge, mobility, and transport behavior of PFOA under high-ionic-strength conditions. However, because ion pairing was not directly measured in the present study, its contribution to PFOA transport cannot be quantified (Du et al., 2014).

3.5.4 High electric field and possible non-ideal transport

At the applied electric field of 4 V/cm, concentration polarization and other non-ideal transport phenomena may influence membrane transport. Because limiting-current behavior was not independently characterized, an overlimiting-current regime cannot be established from the present experiments (Rubinstein and Zaltzman, 2000; Rubinstein and Zaltzman, 2007).

3.5.5 AEM rupture, membrane stability, and non-ideal transport

Real ion-exchange membranes are not perfectly selective, and their transport behavior can be affected by membrane morphology, swelling, fouling, and operating conditions (Probstein and Hicks, 1993; Strathmann, 2004; Steinle-Darling et al., 2008). This may be as a result of partial passage of PFOA across the membrane despite its nominal exclusion properties (Fig 6). Membrane integrity was evaluated after EK–IEM treatment by visual inspection and SEM–EDS characterization. Physical rupture of the AEM was observed, particularly under the high-salinity condition. Because the AEM provides the principal anion-transport pathway, its rupture could reduce membrane selectivity and create a non-selective pathway for $PFOA^-$ and other dissolved ions.

Temperature measurements performed at 1-h intervals showed substantial thermal loading during treatment, with the maximum measured temperature reaching 71.6 °C at 2 h under the high-salinity condition (Tab.7). The occurrence of AEM rupture under this high-temperature, high-current operating condition suggests that thermal loading may have contributed to membrane damage. However, because the temperature at the membrane surface and the membrane mechanical properties were not independently measured, thermal stress cannot be established as the sole cause of failure. The observed AEM rupture therefore provides a plausible and potentially important explanation for the non-ideal PFOA distribution and should be considered when interpreting the transport mechanisms.

Table 6. Measured reactor temperature during EK–IEM treatment under different salinity conditions

Time (h)	Temp LCT (°C)	Temp MCT (°C)	Temp HCT (°C)

0	22.8	21.5	22.3
1	62.8	67.8	65.2
2	48.8	63.8	71.6
3	38.7	41.8	70.6
4	32.2	33	48.4
5	28.5	28.8	37

The persistence of elevated temperature under HCT through 3 h is consistent with the sustained higher current observed under this condition and indicates a greater thermal burden during high-salinity operation. The reported temperatures are bulk/reactor measurements in middle compartment (fig.1).

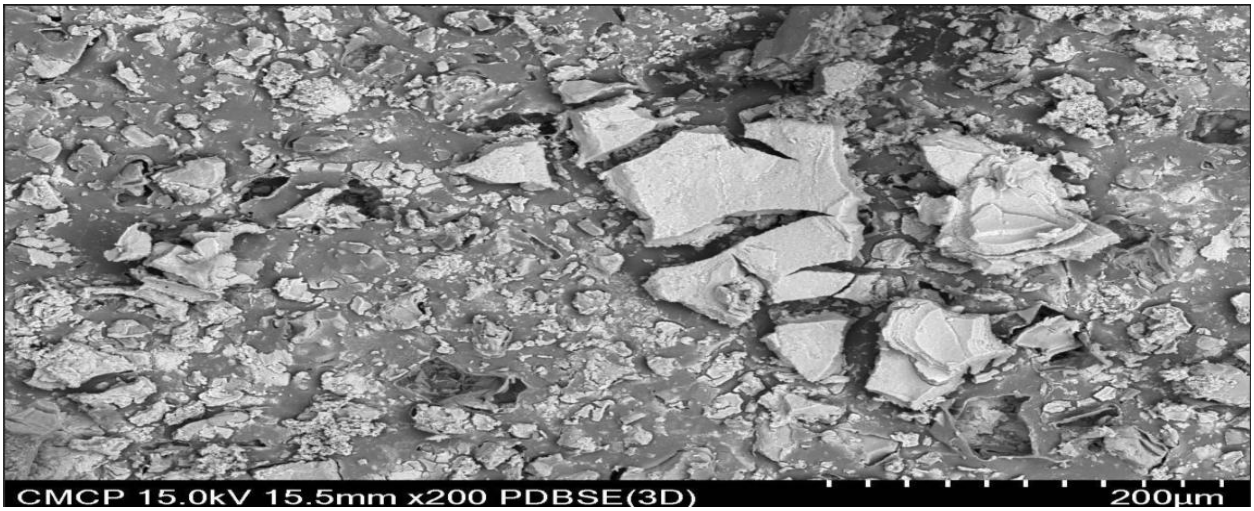


Figure 4. SEM–EDS characterization of the ruptured AEM following high-salinity treatment (HCT), showing morphological damage to the membrane

3.5.6 Influence of pH on PFOA under different salinity conditions

Although PFOA is a weak acid that exists predominantly in its anionic form under most environmentally relevant conditions, local pH changes near the membrane surface may lead to partial protonation. Under sufficiently acidic conditions, partial protonation of PFOA to its neutral form (PFOAH) may occur, and the neutral species may diffuse more readily through the membrane than the charged $PFOA^-$ form (Goss, 2008).

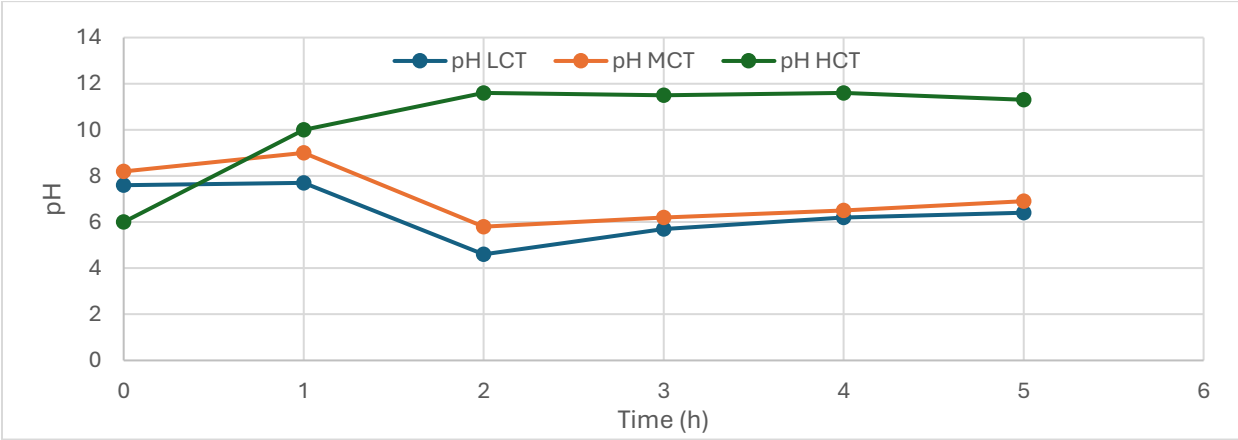


Figure 5. pH variation over 5h for LCT, MCT, HCT

Figure 5 presents the temporal evolution of pH in the centre compartment of the EK–IEM reactor during 5 h of treatment at low-, medium-, and high-salinity conditions (LCT, MCT, and HCT). The results demonstrate that the initial salinity strongly influenced the electrochemical and chemical environment within the reactor. The three conditions exhibited distinctly different pH profiles, indicating that pH evolution was governed by the coupled effects of ionic strength, electrical current, ion migration, and electrochemical water-splitting reactions.

At the beginning of treatment, the centre-compartment pH was approximately 7.5, 8.2, and 6.0 for LCT, MCT, and HCT, respectively. During the first hour, the pH increased to approximately 7.7 for LCT, 9.0 for MCT, and 10.0 for HCT. The initial alkalinization was particularly pronounced under HCT, where the pH increased by approximately 4 units within the first hour. This response coincided with the higher conductivity and current associated with the high-salinity condition, suggesting enhanced electrochemical activity and ion transport under the higher ionic strength.

A pronounced divergence among the treatments occurred between 1 and 2 h. Under LCT and MCT, the centre-compartment pH decreased from approximately 7.7 to 4.6 and from 9.0 to 5.8, respectively. In contrast, HCT continued to increase to approximately pH 11.5. The acidification observed under LCT and MCT indicates a substantial change in the balance of proton and hydroxide transport within the reactor. Under the applied electric field, water-splitting reactions at the electrodes generate H^+ and OH^-, while the ion-exchange membranes regulate the migration of charged species between compartments. Consequently, the measured pH in the centre compartment represents the combined effect of electrochemical generation, membrane-mediated ion transport, and ionic redistribution rather than electrode reactions alone.

After 2 h, the LCT and MCT systems exhibited gradual pH recovery, reaching approximately 6.5 and 6.9, respectively, at 5 h. HCT, however, remained strongly alkaline throughout the remainder of the experiment, with pH values of approximately 11.4, 11.5, and 11.2 at 3, 4, and 5 h, respectively. The persistence of the alkaline condition under HCT suggests that the high-ionic-strength environment established a substantially different electrochemical regime from those observed under LCT and MCT.

The observed pH conditions are also relevant to PFOA transport. Because PFOA is predominantly present in its anionic form under the experimental conditions, changes in pH can influence its speciation and electrokinetic transport behavior. Nevertheless, the present experiments involved simultaneous changes in salinity, conductivity, current, temperature, and pH; therefore, the pH trends alone cannot be used to establish a direct causal relationship with PFOA removal. Rather, they demonstrate that salinity establishes the initial ionic environment, which influences conductivity and current, while the resulting electrochemical processes control pH evolution and consequently contribute to the overall conditions governing PFOA transport and membrane performance.

Overall, Figure 5 demonstrates that increasing salinity substantially altered the pH dynamics of the EK–IEM system. LCT and MCT exhibited transient acidification followed by partial recovery toward near-neutral conditions, whereas HCT underwent rapid and persistent alkalinization. These differences highlight the importance of simultaneously monitoring pH, conductivity, current, and temperature when evaluating EK–IEM treatment of high-salinity produced water, particularly because extreme pH and temperature conditions may affect membrane stability and long-term process operation.

3.5.7 Influence of energy input on transport efficiency

Energy input influenced PFOA removal and the associated transport behavior. At lower cumulative energy input, PFOA removal increased rapidly, whereas further increases in energy produced progressively smaller improvements in removal efficiency. This behavior suggests diminishing treatment returns at higher cumulative energy input. The observed response may be associated with increasing competition from background ions, concentration-polarization effects, and other non-ideal transport processes. Because electroosmotic flow was not independently measured, its contribution to the observed transport behavior cannot be quantified from the present experiments (Zhang et al., 2013; Rahman et al., 2014).

Because PFOA predominantly exists as the negatively charged perfluorooctanoate anion ($PFOA^-$) under most environmentally relevant pH conditions, it is expected to undergo electromigration toward the anode under an applied electric field. However, interactions with multivalent cations may modify the effective transport behavior of PFOA and contribute to deviations from idealized monovalent anion electromigration under saline conditions.

The results therefore suggest that PFOA transport was primarily associated with electromigration under the applied electric field, while increasing salinity and cumulative energy input may have enhanced the influence of ion competition and other non-ideal transport processes. Before membrane failure, the PFOA removal behavior was

consistent with electromigration toward the anode and transport through the AEM; however, membrane rupture may have introduced an additional non-selective pathway.

At higher salinity, the high concentration of chloride and other background anions may have increased competition for anionic transport through the AEM, potentially reducing the relative contribution of PFOA to the total anionic flux (Du et al., 2014; Peng et al., 2020; Jiang et al., 2021). These ions contribute substantially to charge transport and increase the electrical current. The resulting electrochemical and interfacial conditions may also influence electroosmotic flow (EOF), although EOF was not independently measured in the present study. Both $PFOA^-$ and Cl^- are driven toward the anode under the applied electric field, while the high concentration of chloride may reduce the relative transport contribution of $PFOA^-$ through competition for available anion-transport pathways (Appleman et al., 2014; Rahman et al., 2014; Zhang et al., 2019).

Chloride and sulfate were below the analytical detection limits in the catholyte, whereas PFOA was detected under several conditions. This observation suggests that conventional anion electromigration alone may not fully explain the observed PFOA distribution. Possible contributors include electroosmotic water movement, other non-ideal transport processes through the CEM, ion association with counterions, concentration-polarization effects, or localized membrane leakage. However, because these mechanisms were not independently measured, their individual contributions cannot be distinguished from the present experiments.

3.6. Energy Considerations

3.6.1. Influence of current

The DC intensity exhibited a strong dependence on solution salinity, reflecting the influence of ionic strength on solution conductivity and charge transport within the electrokinetic system.

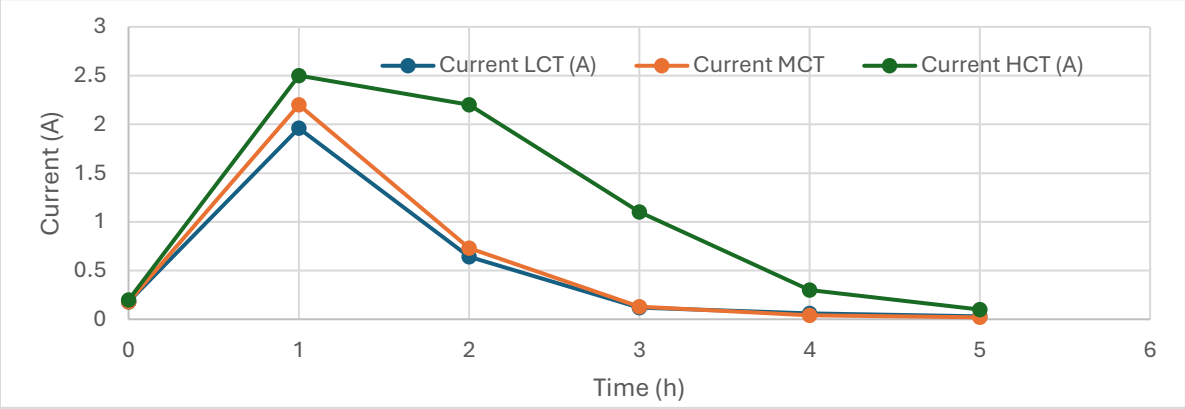


Figure 6a. Temporal evolution of current under LCT, MCT, and HCT conditions

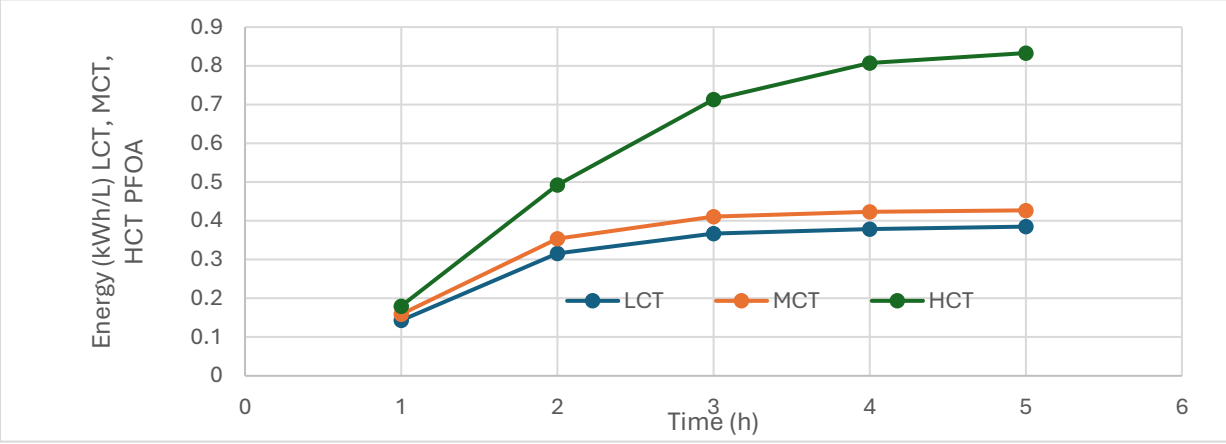


Figure 6b. Specific energy consumption as a function of treatment time under low-, medium-, and high-salinity conditions during EK–IEM treatment.

As show in Fig. 6a, the current increased sharply during the first hour, reaching maximum values of 1.96, 2.20, and 2.50 A for LCT, MCT, and HCT, respectively, followed by a progressive decline throughout the remaining treatment period. The higher initial current under HCT is consistent with its greater ionic strength and conductivity, which provided a larger concentration of mobile charge carriers and reduced the electrical resistance of the treated solution. As treatment proceeded, the progressive removal and redistribution of ionic species resulted in declining conductivity and, consequently, decreasing current. This behavior was particularly evident for LCT and MCT, where the current decreased to 0.03 and 0.02 A, respectively, at 5 h, whereas HCT retained a higher current of 0.10 A.

Despite having the lowest sustained current after the initial treatment stage, LCT achieved the highest PFOA removal (~99.5%), whereas MCT and HCT achieved approximately 96.3% and 97.5% removal, respectively.

The elevated current under HCT also has important thermal implications. Because electrical power dissipation increases with current under the applied voltage, the high initial current promoted substantial Joule heating, consistent with the elevated temperatures observed during the early treatment period. As ion removal progressed, conductivity and current decreased, resulting in reduced heat generation and subsequent cooling of the reactor. Therefore, the current results demonstrate that salinity simultaneously controls the electrical driving force for ion transport and the thermal load imposed on the membrane system. The overall PFOA treatment performance consequently reflects a balance among electrokinetic driving force, competing-ion transport, Joule heating, and membrane stability.

3.6.2 Energy consumption

Specific energy consumption (SEC) was calculated from the cumulative electrical energy supplied to the reactor divided by the treated volume (kWh/L). Electrical energy consumption was determined by integrating the measured current over treatment time at the applied voltage of 40 V (Eqs. 4 and 5). As shown in Fig. 6b, SEC increased progressively with treatment duration under all salinity conditions. For LCT, SEC increased from 0.143 kWh/L at 1 h to 0.385 kWh/L at 5 h, while MCT and HCT reached 0.427 and 0.833 kWh/L, respectively, at 5 h. At 3 h, SEC values were 0.367, 0.411, and 0.713 kWh/L for LCT, MCT, and HCT, respectively, corresponding to approximately 99%, 93%, and 93% PFOA removal. The higher SEC under HCT is consistent with its higher and more sustained current, particularly during the first 3 h. Although current decreased with treatment time, cumulative energy consumption continued to increase. Thus, increasing salinity substantially increased the electrical energy requirement without producing a proportional increase in PFOA removal.

Under the tested conditions, approximately 3 h provided a favorable treatment window for substantial PFOA removal while limiting additional cumulative energy input. Because the experiments were conducted in a 300-mL laboratory-scale batch reactor, the reported SEC values should be interpreted as laboratory-scale results rather than full-scale energy requirements. Pilot- and larger-scale studies are needed to evaluate energy consumption and optimize operating conditions for practical application (Xu et al., 2019; Tshangana et al., 2025).

3.6.3 Relationship between energy consumption and PFOA removal

The increasing separation between the HCT, MCT, and LCT curves is consistent with greater energy demand at higher salinity. At high salinity, chloride and sulfate ions compete strongly with $PFOA^-$ for transport through the anion exchange membrane, leading to lower transport selectivity and higher energy consumption. Furthermore, at high ionic strength, compression of the electrical double layer may reduce electrostatic exclusion and alter effective membrane permselectivity, allowing competing ions to contribute more substantially to the total ionic flux.

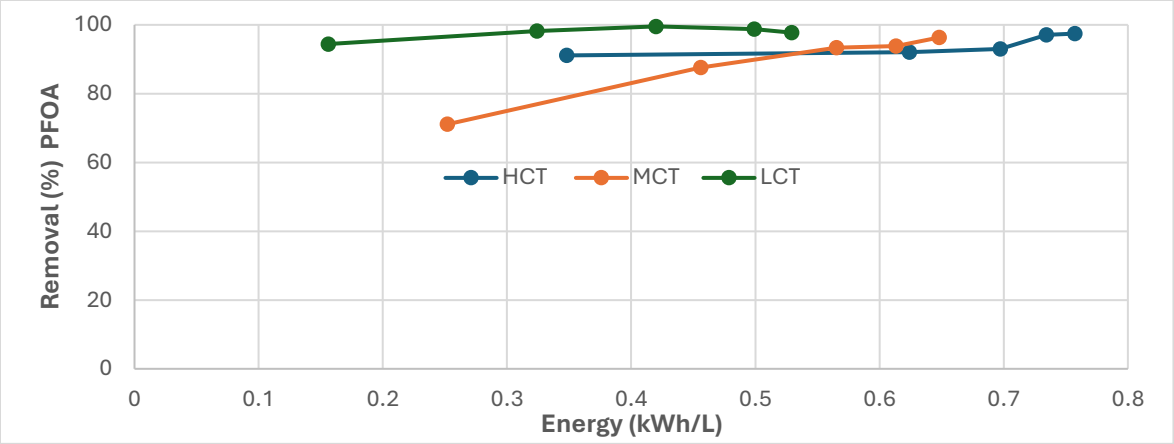


Figure 7. Relationship between specific energy consumption and PFOA removal under low-, medium-, and high-salinity conditions during EK–IEM treatment

The relationship between specific energy consumption (SEC) and PFOA removal differed among the three salinity conditions as shown in Fig. 7. Under LCT, PFOA removal reached approximately 94.4% at 1 h at an SEC of 0.143 kWh/L (143 kWh/m³) and increased to approximately 99.5% at 3 h at 0.367 kWh/L. Further treatment increased SEC to 0.385 kWh/L (385 kWh/m³) at 5 h without improving PFOA removal, which decreased slightly to approximately 97.8%. Under MCT, PFOA removal increased from 71.1% at 1 h to 93.3% at 3 h and 96.3% at 5 h, while SEC increased from 0.159 to 0.411 and 0.427 kWh/L (427 kWh/m³), respectively. Under HCT, PFOA removal increased from 91.1% at 1 h to 93.0% at 3 h and 97.5% at 5 h, whereas SEC increased substantially from 0.180 to 0.713 and 0.833 kWh/L (833 kWh/m³), respectively.

These results demonstrate that increasing energy input does not produce a proportional increase in PFOA removal, particularly under high-salinity conditions. The higher SEC under HCT is associated with the greater and more sustained electrical current resulting from the higher ionic strength of the wastewater. Consequently, an optimum operating period should be established by balancing PFOA removal against energy consumption and membrane stability.

Therefore, these results indicate that treatment time should be selected according to the desired removal target rather than maximized solely to increase removal. Under the tested conditions, approximately 3 h represented a favorable operating window because substantial PFOA removal had already been achieved while additional treatment increased cumulative energy consumption. This observation should not be interpreted as a universal optimum because the experiments were conducted in a laboratory-scale batch reactor at fixed voltage and membrane configuration. Instead, the result demonstrates the need to define a salinity- and energy-dependent operating window for EK–IEM treatment.

3.7 Implications for EK–IEM process optimization

The results demonstrate that salinity controls several interconnected aspects of EK–IEM operation. Increasing salinity increased ionic conductivity and electrical current, but the associated increase in electrical loading also increased energy consumption and thermal burden. At the highest salinity tested, these effects coincided with physical AEM rupture. Therefore, the operating condition cannot be optimized using PFOA removal alone.

The central engineering implication is that EK–IEM treatment of hypersaline wastewater has a coupled transport–energy–stability trade-off. Higher ionic conductivity can sustain electrical transport but can also increase energy demand and thermal loading, while abundant background ions can contribute substantially to total ionic transport. Under the present conditions, approximately 3 h provided a favorable treatment window for substantial PFOA removal without the additional cumulative energy associated with longer operation.

Accordingly, future reactor optimization should use conductivity, current, temperature, treatment time, and PFOA removal as interconnected operating variables. Real-time current and temperature monitoring could provide a practical basis for adjusting applied voltage to limit excessive electrical and thermal loading while maintaining the desired contaminant removal.

Several limitations should be considered when interpreting these findings. PFOA concentrations were estimated using a single-point response factor rather than a multi-point quantitative calibration, and electroosmotic flow and intrinsic membrane transport numbers were not independently measured. In addition, membrane-surface temperature and mechanical properties were not characterized during operation. The experiments were conducted using synthetic produced water in a 300-mL batch reactor. Therefore, the identified transport and membrane-stability relationships should be regarded as experimentally supported trends under the tested conditions rather than universal operating limits.

Table 7. Comparison of PFOA/PFAS treatment approaches and the contribution of the present EK–IEM study

Treatment approach	Target	Matrix	Salinity considered	Main outcome	Main limitation
GAC/adsorption	PFOA/PFAS	Water	Low–moderate	Removal	Spent media
Ion exchange	PFOA/PFAS	Water	Variable	High removal	Regeneration/concentrate
NF/RO	PFOA/PFAS	Water	Variable	High rejection	Concentrate + osmotic pressure
Electrochemical / electrical membrane	PFOA/PFAS	Water	Limited / variable	High removal /rejection	Energy/matrix effects
EK–IEM, this study	**PFOA**	**Produced water**	**10–80 g/L NaCl**	**96.3–99.5% removal**	**Energy + membrane stability at high salinity**

Table 7 shows that established PFAS treatment technologies, including adsorption, ion exchange, NF, and RO, can achieve substantial PFAS removal but may generate spent media or PFAS-concentrated residual streams requiring further management (Mastropietro et al., 2021; Yadav et al., 2022; Tshangana et al., 2025). The present EK–IEM system achieved 96.3%–99.5% PFOA removal from produced water containing 10–80 g NaCl/L. Its principal contribution is therefore the evaluation of PFOA treatment under hypersaline produced-water conditions while simultaneously examining electrical energy demand and membrane stability.

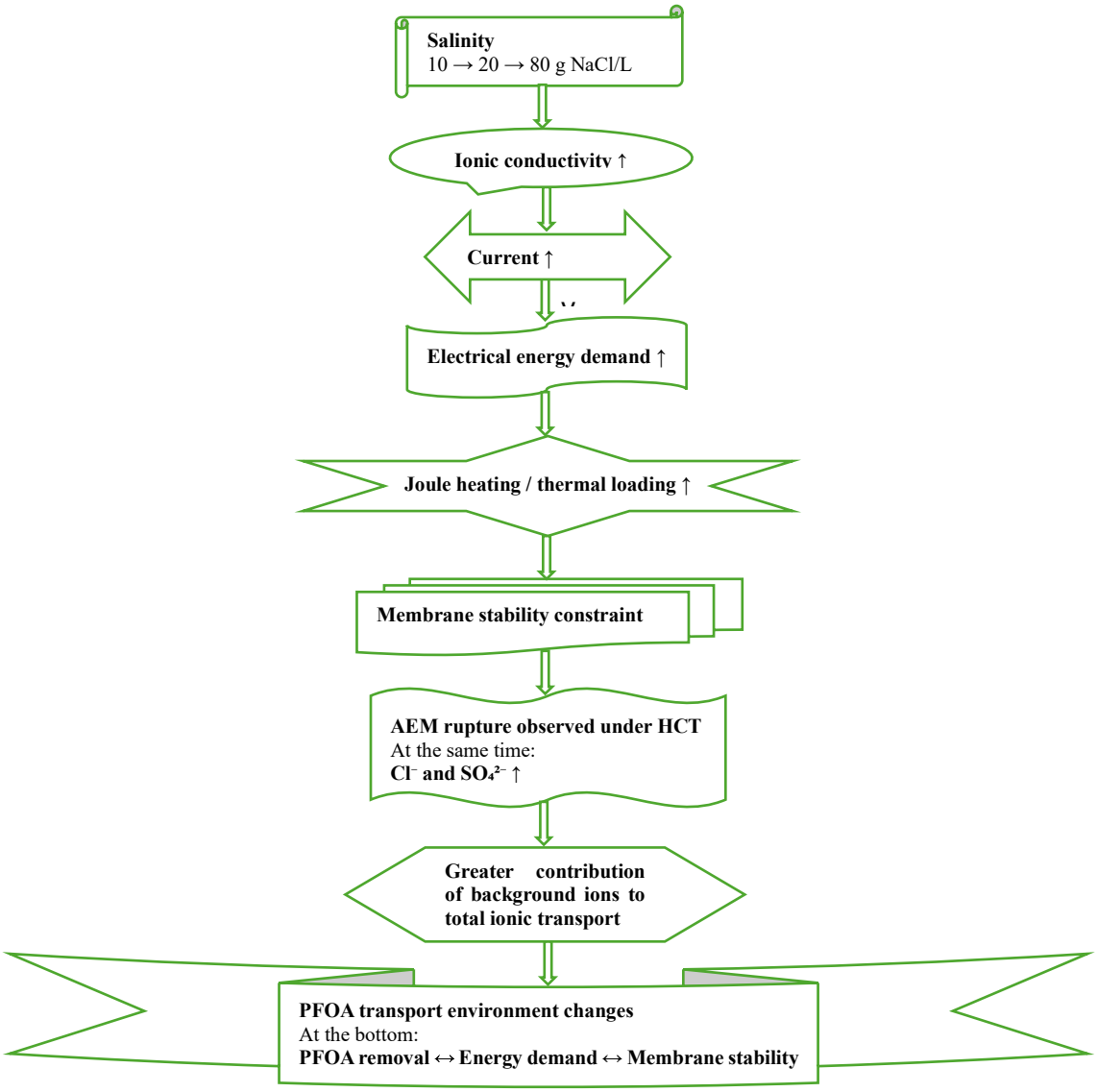


Figure 8. Conceptual framework showing the coupled effects of salinity on PFOA transport, electrical loading, energy consumption, and membrane stability in the EK–IEM system.

Figure 8 summarizes the coupled transport–energy–stability relationship identified in this study. Increasing salinity enhanced ionic conduction and electrical loading but also increased energy demand and thermal burden. The results therefore indicate that optimization of EK–IEM treatment should consider contaminant removal together with electrical energy input and membrane stability.

4. Conclusion

This study demonstrated the potential of a two-stage hybrid electrokinetic–ion exchange membrane (EK–IEM) process for treating PFOA-contaminated produced water across a broad salinity range. The membrane-free electrokinetic pretreatment substantially reduced oil, COD, and turbidity, providing an effective conditioning step before membrane treatment. Subsequent EK–IEM treatment achieved PFOA removals of 99.5%, 96.3%, and 97.5% under low-, medium-, and high-salinity conditions, respectively, demonstrating that substantial PFOA removal can be maintained even in highly saline wastewater.

The results show that salinity is an important operating variable because it simultaneously affects ionic transport, electrical current, energy demand, and thermal loading. PFOA transport was consistent with electromigration of the predominantly anionic species toward the anode through the anion exchange membrane.

However, increasing concentrations of background ions, particularly chloride and sulfate, altered the overall ionic transport environment and reduced the relative contribution of PFOA to charge transport. The observed transport behavior may also have been influenced by concentration polarization, electroosmotic effects, and interactions between PFOA and background ions; however, the individual contributions of these mechanisms could not be quantified from the present experiments.

Overall, the study shows that PFOA removal efficiency alone is insufficient to define the performance of EK–IEM treatment in hypersaline wastewater. Treatment time, electrical energy input, competing-ion transport, thermal loading, and membrane stability must be considered simultaneously. Under the tested laboratory conditions, approximately 3 h provided a favorable operating window for substantial PFOA removal. These findings provide an experimental basis for further development of EK–IEM systems for PFAS treatment in highly saline industrial wastewater.

Acknowledgements

The authors gratefully acknowledge the financial support provided by the Natural Sciences and Engineering Research Council of Canada (NSERC) Discovery grant awarded to Dr. Elektorowicz, grant from the Tertiary Education Trust Fund (TETFund), Nigeria, and the Fonds de recherche du Québec – Nature et technologies (FRQNT), Gina Cody School of Engineering and Computer Science whose support made this research possible.

Funding

No funding was received for conducting this study

Authors' Contributions

1. Emmanuel Mbah: Conceptualization, Methodology, Investigation, Data curation, Formal analysis, Visualization, Writing – original draft, Writing – review and editing.
2. Maria Elektorowicz: Supervision, Methodology, Writing – review and editing.
3. Mehrab Malekshahi Nejad: Formal analysis, Writing – review and editing

All authors read and approved the final manuscript.

Ethical Approval

Not applicable.

Consent to Participate

Not applicable.

Consent to Publish

Not applicable.

Competing Interests

The authors declare no competing interests.

Data Availability Statement

The datasets generated and/or analyzed during the current study are available from the corresponding author upon reasonable request.

References

Acar Y B, Alshawabkeh A N (1993). Principles of electrokinetic remediation. *Environ Sci Technol*, 27(13):2638–2647. doi:10.1021/es00049a002

Al-Maas M, Minier-Matar J, Hussain A, AlShamari E, Sharma R, Adham S (2025). Osmotically assisted reverse osmosis: Assessing pretreatment on hypersaline produced water. *Desalination*, 604:118724. doi:10.1016/j.desal.2025.118724

Appleman T D, Higgins C P, Quinones O, Vanderford B J, Kolstad C, Zeigler-Holady J C, Dickenson E R V (2014). Treatment of poly- and perfluoroalkyl substances in U.S. full-scale water treatment systems. *Water Res*, 51:246–255. doi:10.1016/j.watres.2013.10.067

Ateia M, Maroli A, Tharayil N, Karanfil T (2020). An overview of per- and polyfluoroalkyl substances (PFAS) in the environment: Source, fate, risk and regulations. *Water*, 12(12):3590. doi:10.3390/w12123590

Buck R C, Franklin J, Berger U, Conder J M, Cousins I T, de Voogt P, Jensen A A, Kannan K, Mabury S A, van Leeuwen S P J (2011). Perfluoroalkyl and polyfluoroalkyl substances in the environment: Terminology, classification, and origins. *Integr Environ Assess Manag*, 7(4):513–541. doi:10.1002/ieam.258

Burns D C, Ellis D A (2008). Experimental pKa determination for perfluorooctanoic acid (PFOA) and the potential impact of pKa concentration dependence on laboratory-measured partitioning phenomena and environmental fate. *Environ Sci Technol*, 42(24):9283–9288. doi:10.1021/es802047v

Dixit F, Dutta K, Cooksley C, Madaeni S S (2021). Removal of per- and polyfluoroalkyl substances (PFAS) from water by ion exchange resins: A review. *Chemosphere*, 272:129777. doi:10.1016/j.chemosphere.2021.129777

Du Z, Deng S, Bei Y, Huang Q, Wang B, Huang J, Yu G, Xing B (2014). Adsorption behavior and mechanism of perfluorinated compounds on various adsorbents—A review. *J Hazard Mater*, 274:443–454. doi:10.1016/j.jhazmat.2014.04.038

European Parliament and Council of the European Union (2020). Directive (EU) 2020/2184 of the European Parliament and of the Council of 16 December 2020 on the quality of water intended for human consumption (recast). *Off J Eur Union*, L435:1–62.

Glüge J, Scheringer M, Cousins I T, DeWitt J C, Goldenman G, Herzke D, Lohmann R, Ng C A, Trier X, Wang Z (2020). An overview of the uses of per- and polyfluoroalkyl substances (PFAS). *Environ Sci Process Impacts*, 22(12):2345–2373. doi:10.1039/D0EM00291G

Goss K U (2008). The pKa values of perfluorooctanoic acid and other highly fluorinated carboxylic acids. *Environ Sci Technol*, 42(2):456–458. doi:10.1021/es702192c

Jahromi A F, Elektorowicz M (2018). Electrokinetically assisted oil-water phase separation in oily sludge with implementing novel controller system. *J Hazard Mater*, 358:434–440. doi:10.1016/j.jhazmat.2018.07.032

Jiang S, Sun H, Wang H, Ladewig B P, Yao Z (2021). A comprehensive review on the synthesis and applications of ion exchange membranes. *Chemosphere*, 282:130817. doi:10.1016/j.chemosphere.2021.130817

Kwiatkowski C F, Andrews D Q, Birnbaum L S, Bruton T A, DeWitt J C, Knappe D R, Maffini M V, Miller M F, Pelch K E, Reade A, Soehl A, Trier X, Venier M (2020). Scientific basis for managing PFAS as a chemical class. *Environ Sci Technol Lett*, 7(8):532–543. doi:10.1021/acs.estlett.0c00255

Mastropietro T F, Bruno R, Pardo E, Armentano D (2021). Reverse osmosis and nanofiltration membranes for highly efficient PFASs removal: Overview, challenges and future perspectives. *Dalton Trans*, 50:5398–5410. doi:10.1039/D1DT00360G

Nikonenko V V, Pismenskaya N D, Belova E I, Sistat P, Huguet P, Pourcelly G, Larchet C (2010). Intensive current transfer in membrane systems: Modelling, mechanisms and application in electrodialysis. *Adv Colloid Interface Sci*, 160(1–2):101–123. doi:10.1016/j.cis.2010.08.001

Peng Y, Liu H, Wang Y, Chen Y (2020). Recent advances in electrokinetic remediation technology applied to contaminated soils. *J Hazard Mater*, 400:123230. doi:10.1016/j.jhazmat.2020.123230

Post G B, Cohn P D, Cooper K R (2012). Perfluorooctanoic acid (PFOA), an emerging drinking water contaminant: A critical review of recent literature. *Environ Res*, 116:93–117. doi:10.1016/j.envres.2012.03.007

Probstein R F, Hicks R E (1993). Removal of contaminants from soils by electric fields. *Science*, 260(5107):498–503. doi:10.1126/science.260.5107.498

Rahman M F, Peldszus S, Anderson W B (2014). Behaviour and fate of perfluoroalkyl and polyfluoroalkyl substances (PFASs) in drinking water treatment: A review. *Water Res*, 50:318–340. doi:10.1016/j.watres.2013.10.045

Rubinstein I, Zaltzman B (2000). Electro-osmotically induced convection at a permselective membrane. *Phys Rev E*, 62(2):2238–2251. doi:10.1103/PhysRevE.62.2238

Rubinstein I, Zaltzman B (2007). Electro-convective versus electroosmotic instability in concentration polarization. *Adv Colloid Interface Sci*, 134–135:190–200. doi:10.1016/j.cis.2007.04.013

Salih H H M, Huggett E, Patterson C, Scott J, Gune Silva R, Lee T, Speth T F, Nadagouda M N (2026). Treatment of per- and polyfluoroalkyl substances (PFAS)-contaminated hypersaline brine by membrane distillation. *ACS Environ Au*, 6(1):66–73. doi:10.1021/acsenvironau.5c00008

Steinle-Darling E, Du P, Reinhard M (2008). NF and RO for PFAS removal. *Environ Sci Technol*, 42(14):5292–5297.

Strathmann H (2004). *Ion-exchange membrane separation processes*. Amsterdam: Elsevier.

Strathmann H (2010). Electrodialysis, a mature technology with a multitude of new applications. *Desalination*, 264(3):268–288. doi:10.1016/j.desal.2010.04.069

Taher M N, Al-Mutwalli S A, Barisci S, Koseoglu-Imer D Y, Dumée L F, Shirazi M M A (2024). Progress on remediation of per- and polyfluoroalkyl substances (PFAS) from water and wastewater using membrane technologies: A review. *J Water Process Eng*, 59:104858. doi:10.1016/j.jwpe.2024.104858

Tshangana C S, Nhlengethwa S T, Glass S, Denison S, Kuvarega A T, Nkambule T T I, Mamba B B, Alvarez P J J, Muleja A A (2025). Technology status to treat PFAS-contaminated water and limiting factors for their effective full-scale application. *npj Clean Water*, 8:41. doi:10.1038/s41545-025-00457-3

U.S. Environmental Protection Agency (2021). *Method 533: Determination of PFAS in drinking water by isotope dilution anion exchange solid phase extraction and LC-MS/MS*. Washington, DC: U.S. Environmental Protection Agency.

U.S. Environmental Protection Agency (2024). National primary drinking water regulation for certain per- and polyfluoroalkyl substances (PFAS): Final rule. *Fed Regist*, 89(80):32532–32720.

Veil J A, Puder M G, Elcock D, Redweik R J (2004). *A white paper describing produced water from production of crude oil, natural gas, and coal bed methane*. U.S. Department of Energy, National Energy Technology Laboratory.

Xu L, Yu Y, Sang W, Wu L (2019). Produced water treatment technologies and their applicability under different field conditions. *J Pet Sci Eng*, 176:794–806. doi:10.1016/j.petrol.2019.02.057

Yadav S, Ibrar I, Al-Juboori R A, Singh L, Ganbat N, Kazwini T, Karbassiyazdi E, Samal A K, Subbiah S, Altaee A (2022). Updated review on emerging technologies for PFAS contaminated water treatment. *Chem Eng Res Des*, 182:667–700. doi:10.1016/j.cherd.2022.04.009

Zhang C, Yan H, Li F, Hu X, Zhou Q (2013). Sorption of short- and long-chain perfluoroalkyl surfactants on sewage sludges. *J Hazard Mater*, 260:689–699. doi:10.1016/j.jhazmat.2013.06.022

Zhang K, Crittenden J C (2024). Electrochemical adsorption of perfluorooctanoic acid from aqueous solutions using ion exchange membranes. *J Water Process Eng*, 59:104872. doi:10.1016/j.jwpe.2024.104872

Zhang Y, Chen J, Zhang D, Yan Z, Zhou Q (2019). Electromigration and transport behavior of perfluorooctanoic acid in saturated porous media under electric fields. *J Hazard Mater*, 364:38–46. doi:10.1016/j.jhazmat.2018.09.088